IOP Publishing Journal of Physics: Condensed Matter

J. Phys.: Condens. Matter **22** (2010) 084019 (11pp) doi:10.1088/0953-8984/22/8/084019

Thin film evolution equations from (evaporating) dewetting liquid layers to epitaxial growth

U Thiele[1]

Department of Mathematical Sciences, Loughborough University, Leicestershire LE11 3TU, UK

E-mail: u.thiele@lboro.ac.uk

Received 1 October 2008, in final form 6 November 2008
Published 5 February 2010
Online at stacks.iop.org/JPhysCM/22/084019

Abstract

In the present contribution we review basic mathematical results for three physical systems involving self-organizing solid or liquid films at solid surfaces. The films may undergo a structuring process by dewetting, evaporation/condensation or epitaxial growth, respectively. We highlight similarities and differences of the three systems based on the observation that in certain limits all of them may be described using models of similar form, i.e. time evolution equations for the film thickness profile. Those equations represent gradient dynamics characterized by mobility functions and an underlying energy functional.

Two basic steps of mathematical analysis are used to compare the different systems. First, we discuss the linear stability of homogeneous steady states, i.e. flat films, and second the systematics of non-trivial steady states, i.e. drop/hole states for dewetting films and quantum-dot states in epitaxial growth, respectively. Our aim is to illustrate that the underlying solution structure might be very complex as in the case of epitaxial growth but can be better understood when comparing the much simpler results for the dewetting liquid film. We furthermore show that the numerical continuation techniques employed can shed some light on this structure in a more convenient way than time-stepping methods.

Finally we discuss that the usage of the employed general formulation does not only relate seemingly unrelated physical systems mathematically, but does allow as well for discussing model extensions in a more unified way.

(Some figures in this article are in colour only in the electronic version)

1. Introduction

Structure formation at interfaces and surfaces occurs widely in our natural and technological environment. The spectrum of related phenomena ranges from growing dendrites in solidification or crystallization to budding membranes in the biological cell. Technological processes based on, or affected by, interfacial structuring processes involve, for instance, the sputtering of solid surfaces (that may roughen), the usage of instabilities in the epitaxial growth of nano- or quantum dots, the structuring of homogeneous liquid or elastic coating layers, the deposition of structured nanoparticle assemblies employing instabilities and heat-exchanger technology based on transfer enhancement by surface waves on falling liquid films. A selection is discussed in [1].

Part of the mentioned structuring processes can be modelled as an evolution in time of a surface profile. Models are normally based either on a stochastic microscopic discrete or a deterministic mesoscopic or macroscopic continuum approach. For an overview of methods for the modelling of (solid) nanostructures see [2]. Here, we focus on the continuum approach. There exists an important subset of systems that evolve towards an equilibrium state corresponding to an energetic minimum, i.e. normally these are relaxational systems without any external forcing.

A continuum description of relaxational systems can often be brought into the form of time evolution equation(s) for one

[1] homepage: http://www.uwethiele.de

or several conserved or non-conserved order parameter fields $\phi(\mathbf{x}, t)$ (cf [3]). A non-conserved field might still follow, in part, a conserved dynamics. The dynamics is governed by the underlying energy functional $F[\phi]$. The simplest form for a time evolution of a purely dissipative system without any inertial Hamiltonian dynamics corresponds to the gradient dynamics

$$\partial_t \phi = \nabla \cdot \left[M_c \nabla \frac{\delta F}{\delta \phi} \right] - M_{nc} \frac{\delta F}{\delta \phi} \tag{1}$$

with the $M_c(\phi) \geqslant 0$ and $M_{nc}(\phi) \geqslant 0$ being the mobility functions for the conserved and non-conserved parts of the dynamics, respectively. Here and in the following ∂_t and ∂_x denote partial derivatives w.r.t. time and space, respectively.

A typical example is the Cahn–Hilliard equation describing the demixing of a binary mixture, i.e. a purely 'conserved dynamics' ($M_{nc} = 0$) [4, 5, 3]. Another example is the Allen–Cahn equation describing, for instance, the dynamics of the Ising model in the continuum limit [3]. Multiplying equation (1) by $\delta F/\delta \phi$ and integrating one obtains after a partial integration

$$\frac{\mathrm{d}F[\phi]}{\mathrm{d}t} = -\int M_c \left(\nabla \frac{\delta F}{\delta \phi} \right)^2 \mathrm{d}V - \int M_{nc} \left(\frac{\delta F}{\delta \phi} \right)^2 \mathrm{d}V \leqslant 0 \tag{2}$$

confirming $F[\phi]$ to be a Lyapunov functional.

In the context of evolving surfaces or interfaces, such an equation appears in various contexts. We will discuss here (i) film thickness equations for films of non-volatile and volatile liquids on solid substrates and (ii) surface profile equations for epitaxial growth.

Equation (1) might describe the evolution of the surface profile of an evaporating or condensing thin liquid film on a solid substrate under the influence of capillarity and wettability. In this case, the function $\phi(\mathbf{x}, t)$ represents the film thickness profile and the functional $F[\phi]$ is given by

$$F[\phi] = \int \left[\frac{\gamma}{2} (\nabla \phi)^2 + f(\phi) - \mu \phi \right] \mathrm{d}V \tag{3}$$

where γ is the liquid–gas surface tension and $f(\phi)$ is a local free energy, related to the disjoining pressure $\Pi(\phi)$ by $\Pi = -\partial_\phi f(\phi)$. The term $\mu\phi$ represents an overall energy bias towards the liquid or gaseous state. It is solely responsible for evaporation/condensation of flat 'bulk' films, i.e. films that are thick compared to the range of the disjoining pressure. μ corresponds to a chemical potential. For details and specific choices for the disjoining pressure see, e.g., [6–11].

For Poiseuille flow in the film without slip at the substrate the mobility for the conserved part is $M_c = \phi^3/3\eta$, where η is the dynamic viscosity. Several slip regimes might be accounted for by different choices for $M_c(\phi)$ [12]. The mobility function for the non-conserved part is normally assumed to be a constant (see [13]). Note that there exists an ongoing discussion regarding the form of the non-conserved part of the dynamics (cf, e.g., [14–17, 13, 18]).

Equation (1) with (3) is extensively studied in the conserved case, i.e. for non-volatile films ($M_{nc} = 0$). It can easily be derived from the Navier–Stokes equations and appropriate boundary conditions at the substrate and the free surface employing a long-wave or lubrication approximation [9, 11]. Depending on the particular physical situation studied many different forms for the local energy function $f(\phi)$ are encountered. Beside 'proper' disjoining pressures that model effective molecular interactions between film and substrate (wettability) [19, 20, 6, 7, 21–23, 10, 24] the equations may as well incorporate other pressures modelling, e.g., the influence of an electric field on a film of dielectric liquid in a capacitor [25–29] or films on homogeneously heated substrates that form structures due to a long-wave Marangoni instability [14, 30–34]. The latter is especially interesting because it represents a system that is kept permanently out of equilibrium but is nevertheless described by a gradient dynamics. Note that the situation is slightly different in a closed two-layer system [35] that can, in two dimensions, be described by equation (1) with an appropriate $F[\phi]$ but not in three dimensions.

The above-mentioned Cahn–Hilliard equation describing the conserved dynamics of demixing of a binary mixture corresponds to equations (1) and (3) with a constant M_c, $M_{nc} = 0$ and $f(\phi)$ being a symmetric double well potential. As a consequence, many results obtained for the decomposition of a binary mixture have a counterpart in the dewetting of thin films and vice versa. The analogy was first noted by Mitlin [8] resulting in the notion of 'spinodal dewetting'. Note that there exist other choices for $f(\phi)$ and M_c in the Cahn–Hilliard equation [36, 37]. Equations of similar form may as well model the epitaxial evolution of surfaces of crystalline solids [38–40, 2]. We illustrate this by employing one of the local models for Stranski–Krastanov growth found in the literature—namely a simplified 'glued wetting-layer model' (for details and derivation see [40] (equations (18)–(20)) and [41]). The model assumes an isotropic wetting energy of the epitaxial film on the solid substrate, which is added to the (anisotropic) surface energy. Elastic stresses act through a destabilizing surface stiffness term. It is furthermore assumed that a given amount of material is deposited on the surface that then rearranges in a process of self-organization that might lead to the creation of nano- or quantum dots, i.e. localized surface structures on the nanometre length scale. In the case of high-symmetry orientations of a crystal with cubic symmetry the evolution of the surface profile $\phi(\mathbf{x}, t)$ is described by equation (1) when using a small-slope approximation. As the amount of material is fixed only the conserved part contributes, i.e. $M_c > 0$ and $M_{nc} = 0$. The model in [40] employs a constant mobility M_c (corresponding to a constant surface diffusion coefficient). Non-constant mobilities might as well be used. Note that a fourth-order kinematic term is omitted in the evolution equation as it can lead to artefacts if the slope of the interface is large (inside the small-slope approximation; for details see [41]). The free energy functional is

$$F[\phi] = \int \left[-\frac{\sigma}{2} (\nabla \phi)^2 + \frac{\nu}{2} (\Delta \phi)^2 + \frac{a}{12} (\nabla \phi)^4 + f(\phi) - \mu \phi \right] \mathrm{d}V \tag{4}$$

where $\sigma > 0$ is the destabilizing surface stiffness resulting from elastic stresses, $\nu > 0$ represents the energetic cost of corners and edges, and a quantifies the slope-dependent anisotropic surface energy (note that we fixed the b of [40] as $b = a/3$ to simplify the equation for the present purpose of comparison). The local free energy $f(\phi) = \int W_0(\phi)\,\mathrm{d}\phi$ results from the wetting interaction. Thereby $W_0 = -w(\phi/\delta)^{-\alpha_w}\exp(-\phi/\delta)$, where δ is a characteristic wetting length, and the positive w and α_w characterize the strength and singularity of the underlying interactions. The singularity ensures the stability of the stable monolayer between surface elevations in Stranski–Krastanov growth. Without wetting interactions the epitaxial film would show Volmer–Weber growth, i.e. growth would occur in separated islands not connected by a wetting layer. Note that we here add the last term to equation (4) where μ is the chemical potential. It does not affect the evolution equation when $M_{\mathrm{nc}} = 0$. Related (in part non-local) equations are employed in [42, 43, 2, 44–46].

If vapour deposition is used to deposit the epitaxial layer it is to be expected that equation (1) with (4) and $M_{\mathrm{nc}} > 0$ well describe the process. We are, however, not aware of such an approach in the literature. Actually, for large chemical potential μ as compared to the other terms in F (equation (4)) one can even use the system to describe the evolution under vertical deposition of material. The constant $M_{\mathrm{nc}}\mu$ does then correspond to the constant deposition rate in other models (V in [38]).

Although the overall form of the equation is identical for the various problems introduced above, the specific physics is very different. However, one can still employ the same set of techniques to analyse the various models. Normally, one uses (i) a linear stability analysis of homogeneous steady states, i.e. flat films, to determine the stability of the system and typical length scales that will dominate the short-time evolution in case the homogeneous state is unstable. (ii) Depending on the properties of the dispersion relation obtained in the linear stability analysis one might be able to analytically study stable and unstable steady state solutions and their stability in the weakly nonlinear regime. This is, however, often not possible. (iii) In the strongly nonlinear regime steady states and their stability might still be obtained, e.g. using continuation techniques [47, 48]. These are readily available for two-dimensional systems that can be expressed as ordinary differential equations [49]. Recently, they were also introduced for the full three-dimensional problem, in particular for equation (1) with $M_{\mathrm{nc}} = 0$ and (3) [50]. Note that variational methods are apt to obtain the steady states directly from the functional F, but are not suitable to discuss the stability of the steady states as this involves dynamic aspects. Many groups prefer to 'skip' step (iii) and rather directly (iv) simulate the evolution equation in time using advanced numerical techniques (spectral, pseudo-spectral or semi-implicit).

We remark here that other types of continuum description exist for all the mentioned systems. Whereas here we focus on evolution equations for surface or interface profiles, another class of models describes an interface evolution using phase fields [51]. See, for instance, for dewetting and liquid films/drops in general [10] and for epitaxial growth [52, 43, 2]. We do entirely exclude from our consideration the vast literature on discrete stochastic models that exist for dewetting/evaporation processes (e.g. [53–55]) as well as for surface growth (for reviews see, e.g., [56, 57]).

In the following, we restrict ourselves to two-dimensional physical situations described by film thickness profiles $\phi(x,t)$ that depend on one spatial coordinate only. The drops or quantum dots in 2d will actually refer to liquid ridges or quantum wires in 3d, respectively. We will perform a basic analysis of linear stability and steady states 'in parallel' for a dewetting liquid film on a solid substrate (section 2), a dewetting evaporating/condensing liquid film on a solid substrate (section 3) and the epitaxial structuring of a solid film (section 4). Note that we only review steps (i) and (iii) of the above introduced scheme that sketches a more complete analysis of the system behaviour. The next step would be to use advanced numerical techniques to simulate the evolution of the films in time for two- and three-dimensional physical settings. It involves a rather large number of techniques and groups and we would like to refer the reader to the individual publications cited in the respective sections below.

Before we start we would like to point out the relevance of stable and unstable steady state solutions for systems that evolve in time. Most steady state solutions are either not linearly stable or do not correspond to the global energetic minimum that the system will finally approach. Such solutions are normally not well appreciated in the literature as they are not present 'in equilibrium'. They are, however, often present for a long time in the course of the time evolution and, due to their character as saddles in function space, they do often 'structure' the evolution towards equilibrium. Their stability properties (i.e. growth and relaxation rates) determine timescales for important steps of the dynamics and, as important transients in experiments of finite duration they might actually even get 'frozen in' or 'dried in' as, for example, in the dewetting of thin polymer films [58, 59] or suspensions [60, 61], respectively. In this connection, coarsening, is a particularly interesting issue as in its course the system 'passes through' an infinite number of steady state solutions that are stable when taking their typical size as a reference size, but are unstable with respect to modes on larger length scales, i.e. with respect to coarsening. One could say the individual solutions do first 'attract a time evolution' and then 'expel it' along the single unstable direction (corresponding to coarsening).

2. Dewetting

A dewetting film of non-volatile liquid on a solid substrate is modelled by equations (1) and (3) with $M_{\mathrm{nc}} = 0$ [8, 9, 11]. The local energy $f(\phi)$ corresponds to a disjoining pressure $\Pi(\phi) = -\partial_\phi f(\phi)$ [19, 6, 7]. Various functional forms are used for $f(\phi)$. The particular choice is, however, not very relevant for the qualitative behaviour of the system. The latter only depends on the number and relative depth/height of the extrema of $f(\phi) - \mu\phi$. We choose here $f(\phi) = -\kappa[1/(2\phi^2) - b^3/(5\phi^5)]$ as derived by Pismen from a modified

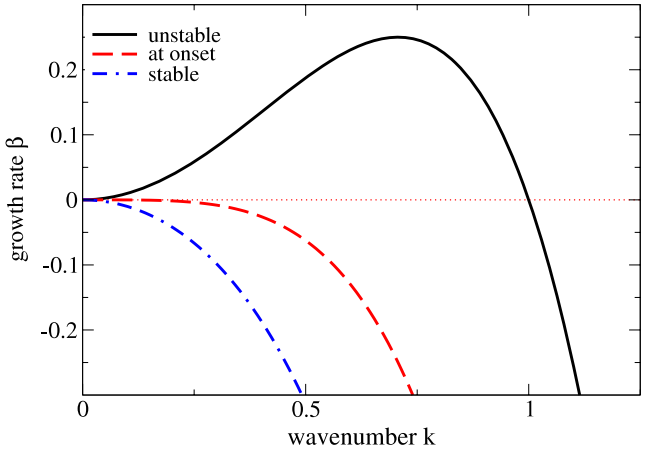

Figure 1. Dispersion relations for the instability of a flat liquid film w.r.t. surface modulations resulting in dewetting and the evolution of patterns of droplets. Shown is a stable and an unstable case in the generic form $\beta = -k^2(k^2 - k_c^2)$, i.e. the growth rate β is scaled by $M_c^0\,\gamma$. The wavenumber is given in units of k_c.

Lennard-Jones potential with hard-core repulsion [62–64]. The resulting $f(\phi)$ has only one minimum at a finite $\phi_{\text{precursor}} = b$. The parameter κ corresponds to a typical energy scale. With the chosen signs the first term corresponds to a destabilizing long-range van der Waals interaction (i.e. κ is proportional to a Hamacker constant) whereas the second one represents a short-range stabilizing interaction. As a consequence, the model may describe drops of a partially wetting liquid in coexistence with a precursor film of thickness b. In the following we scale ϕ by the precursor film thickness, i.e., we fix $b = 1$.

If there existed a second minimum at larger finite thickness it would correspond to a critical height for the transition between spherical-cap-like drops and pancake-like drops (e.g. the capillary length when gravity is included) [6, 65]. For a selection of other pressure terms see, e.g., [6, 66, 10, 67, 8, 68, 69, 60, 70, 59].

Inspecting equation (1) with $M_{\text{nc}} = 0$ one notes that any flat film (thickness $\phi = \phi_0$) corresponds to a steady state solution of the system. However, those films might not be stable. We linearize the system about the flat film employing harmonic modes, i.e. $\phi(x,t) = \phi_0 + \epsilon\,\exp(\beta t + \mathrm{i}kx)$, where $\epsilon \ll 1$ is the smallness parameter and β the growth rate of the harmonic mode of wavenumber k. Entering this ansatz in equation (1) with (3) gives the dispersion relation

$$\beta(k) = -M_c^0\gamma k^2\,(k^2 - k_c^2), \tag{5}$$

where $M_c^0 = M_c(\phi = \phi_0)$. The critical wavenumber is given by $k_c = \sqrt{-\partial_{\phi\phi} f|_{\phi=\phi_0}/\gamma}$. For $\partial_{\phi\phi} f|_{\phi=\phi_0} < 0$ the film is linearly unstable for $0 < k < k_c$. The most dangerous instability mode, i.e. fastest growing mode, has $k_{\max} = k_c/\sqrt{2}$ and $\beta_{\max} = M_c^0\gamma k_c^4/4$. The onset of the instability occurs at $\partial_{\phi\phi} f|_{\phi=\phi_0} = 0$ with $k_c^{\text{onset}} = 0$, i.e. it is a long-wave instability. Note that mass conservation implies $\beta(k = 0) = 0$. Examples of dispersion relations above and below the instability threshold are given in figure 1.

Steady film thickness profiles are obtained by solving equation (1) with $\partial_t\phi = 0$. Note that in the present setting this corresponds to $\delta F/\delta\phi = 0$ because the first integration constant (when integrating equation (1)) is zero as we look at systems without large-scale mean flow. The whole solution structure might be mapped out in parameter space employing continuation techniques using analytically or numerically known solutions to start the continuation [47–49, 11]. Many parameters might be used as main continuation parameter, e.g., period or domain size, film thickness, or any parameter of the energy. Here we only use system size. For a more detailed explanation of the continuation proceedure for thin film equations see the appendices of [71, 72].

For a linearly unstable film a one parameter family of periodic film profiles bifurcates from the flat film at wavenumber k_c as illustrated in figure 2. At the bifurcation point a steady harmonically modulated surface profile exists with a period of $2\pi/k_c$ and an infinitesimally small amplitude. Using period as main continuation parameter the whole family of periodic solutions can be obtained. A selection of resulting film thickness profiles is given in figure 3. We characterize solutions by their norm $||\delta\phi|| = [(1/L)\int_0^L(\phi(x) - \phi_0)^2\mathrm{d}x]^{1/2}$ and energy per length $E = (1/L)\int_0^L F[\phi]\,\mathrm{d}x$. Note that mass

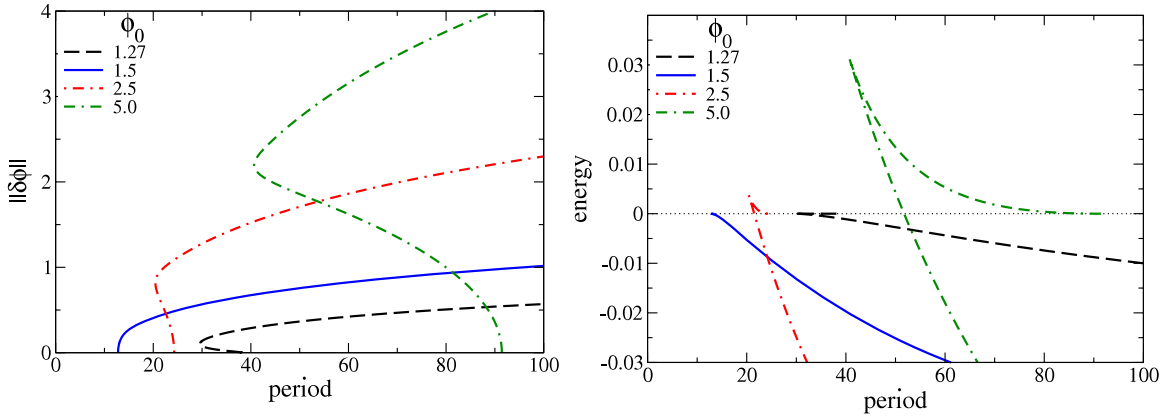

Figure 2. Shown are characteristics of families of steady one-dimensional droplet structures arising in dewetting of a non-volatile liquid using a simple disjoining pressure. The left panel gives the L_2-norm $||\delta\phi||$ and the right one the energy F (equation (3)) per length. The legends give the corresponding mean film thicknesses. The families are obtained using continuation techniques. Note that the solutions are unstable w.r.t. coarsening.

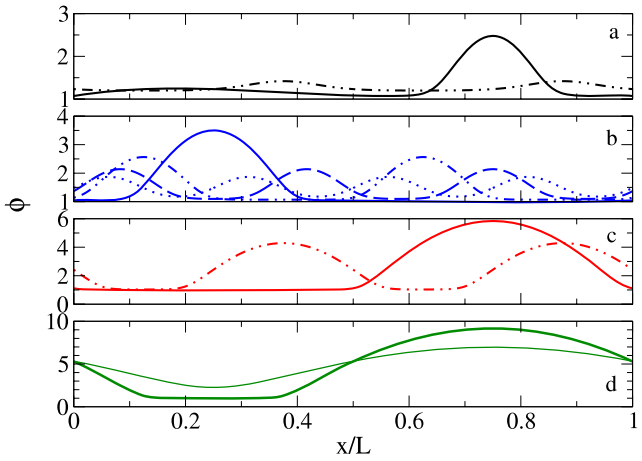

Figure 3. Shown are examples of film thickness profiles for the various branches presented in figure 2. Mean thicknesses $\bar{\phi}$ are (a) 1.27, (b) 1.5, (c) 2.5 and (d) 5.0. The system size is $L = 60$ in all cases. Given are profiles from the following branches: $n = 1$ (solid lines), $n = 2$ (dotted–dashed lines), $n = 3$ (dashed line), and $n = 4$ (dotted line). The thin line in (d) corresponds to a nucleation solution. For given L only the $n = 1$ profiles are stable w.r.t. coarsening.

conservation advises us to directly compare only profiles of identical mean film thickness. This is ensured by μ acting as a Lagrange multiplier. In consequence, μ changes along the individual branches in such a way that the mean of $\phi(x)$ is kept fixed.

The resulting branches might bifurcate from the trivial solution supercritically, i.e., they bifurcate towards the region of the linearly unstable flat film (forward towards larger periods; see, e.g., in figure 2 curve for $\phi_0 = 1.5$). Or the branch bifurcates subcritically, i.e., it emerges towards the region of the linearly stable flat film (backward towards smaller periods; see, e.g., in figure 2 curves for $\phi_0 = 1.27, 2.5$, or 5.0). The location of the border between sub-and supercritical behaviour can be determined employing a weakly nonlinear analysis and can be expressed as an algebraic condition for the 2nd, 3rd and 4th derivative of $f(\phi)$ [73].

In the case of the subcritical bifurcation, the subcritical branch (i.e., between the bifurcation and the saddle-node bifurcation where it 'folds back' towards larger periods) consists of unstable, nucleation solutions that aquire an importance for the rupture process of the film if the system is noisy or 'dirty': Note that for the chosen potential $f(\phi)$ there exist no metastable films. However, one may distinguish two thickness ranges within the linearly unstable range: (i) the linearly unstable modes are fast and will dominate the time evolution even in the presence of defects (finite size perturbations); (ii) the linear modes are slow, and defects—if there are any present—will dominate the time evolution. The distinction is related to the existence of the subcritical branch of unstable solutions. They correspond to nucleation or threshold solutions as they have to be overcome to break the film into drops smaller than the critical wavelength of the linear instability. As they are saddles in function space they can 'organize' the evolution of defect-ridden thin films by offering a fast track to film rupture. This allows to determine a typical time for nucleation events even inside the linear unstable regime and finally to distinguish the nucleation-dominated and instability-dominated behaviour of linearly unstable thin films [74, 24]. A detailed account and comparison to the results of [75] is found in [76]. Note that similar ideas have since been applied to the break-up of liquid ribbons [77]. Recently we also performed a more detailed analysis for a three-dimensional systems [50, 78].

For unstable flat films of thicknesses ϕ_0 the respective branches of solutions bifurcating at $L_c = 2\pi/k_c$ shown in figure 2 are only the first of a respective infinite number of primary solution branches. These bifurcate at domain sizes $L_{cn} = 2\pi n/k_c$, $n = 1, 2, \ldots$. The branch bifurcating at L_{cn} consists of the $n = 1$ branch 'stretched in L' by a factor n. The actual thickness profiles of the n branch consist of n identical drops. This representation of the periodic solutions in dependence on domain size might seem pointless for the present problem. The reason is that the different branches are entirely decoupled. As the situation changes strongly when either looking at other energy functionals (see below section 4), or when breaking the reflection or translational symmetry of the system (by including a lateral driving force [79, 65, 34], substrate heterogeneity [71], or lateral boundary conditions [80]), it is, however, useful to introduce the various branches here.

The monotonic decrease of energy (on the low energy branch) with system size indicates that the system tends to coarsen towards larger and larger structure size. The steady solutions on the 'stable' branches (the branches of drop solutions that continue towards infinite period) are stable when looked at in a domain of the size of their period, but unstable on larger domains, i.e. they are saddles in function space that form the 'stepping stones' of the coarsening process. They first 'attract the time evolution' and then 'expel it' along the only unstable direction (corresponding to coarsening). The coarsening behaviour for a dewetting film is discussed in more detail in [81–84]. Related results for the Cahn–Hilliard equation are discussed, for example, in [3, 85, 86].

Note that results on the nonlinear stability of flat films and the related steady state solutions on branches not connected to the trivial flat film solutions are not discussed here (but see [76, 34, 11]). For discussions of the evolution in the time of dewetting films in two- and three-dimensional settings we refer the reader to [9, 22, 32, 87, 88, 33, 75, 27, 77, 50]. Note finally that continuation may not only be used to obtain families of steady or stationary profiles [70, 65, 72, 73, 89], but as well to track their stability and bifurcations [90, 34, 91, 92].

3. Evaporation

When including evaporation in the presently studied framework one uses equation (1) with the energy functional (3) and $M_{nc} \neq 0$. One notes that, unlike the case without evaporation, flat films of arbitrary thickness $\phi = \phi_0$ do not correspond to a steady state solution of the system any more. However,

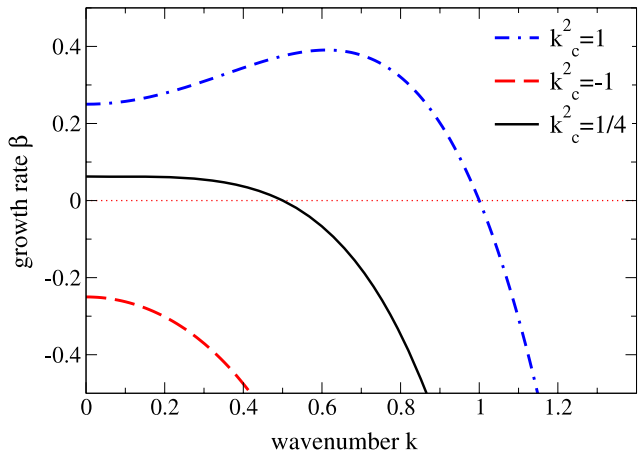

Figure 4. Dispersion relations for the instability of a flat volatile liquid film w.r.t. surface modulations resulting in the evolution of a pattern of droplets. Shown are three qualitatively different cases in the generic form $\beta = -(k^2 + M^0_{\rm nc}/M^0_{\rm c})\,(k^2 - k_{\rm c}^2)$, i.e. we fix $\gamma M^0_{\rm c} = 1$. We furthermore choose $M^0_{\rm nc}/M^0_{\rm c} = 1/4$.

steady flat film solutions still exist when wettability and evaporation balance. For a given chemical potential the corresponding steady thicknesses are given by

$$\partial_\phi f|_{\phi=\phi_0} = \mu, \tag{6}$$

i.e. for the disjoining pressure used here $\phi_0 = [\kappa(1 \pm (1 - 4b^3\mu/\kappa)^{1/2})/2\mu]^{1/3}$. For condensation ($\mu > 0$) two such equilibria exist if $\mu < \kappa/4b^3$ whereas for evaporation ($\mu < 0$) only one thickness exists. Note that this might be different for qualitatively different disjoining pressures like the one used in [13]. As above the steady films might be unstable.

We linearize equation (1) with (3) about the flat film of thickness ϕ_0 given by equation (6) employing harmonic modes as above to obtain the dispersion relation

$$\beta(k) = -M^0_{\rm c}\,\gamma\left(k^2 + \frac{M^0_{\rm nc}}{M^0_{\rm c}}\right)(k^2 - k_{\rm c}^2) \tag{7}$$

where $M^0_{\rm nc} = M_{\rm nc}(\phi = \phi_0)$, $M^0_{\rm c} = M_{\rm c}(\phi = \phi_0)$ and $k_{\rm c} = \sqrt{-\partial_{\phi\phi} f|_{\phi=\phi_0}/\gamma}$ as without evaporation. As the expression in the first parentheses is always positive the film is linearly unstable for $\partial_{\phi\phi} f|_{\phi=\phi_0} < 0$ in the wavenumber range $0 < k < k_{\rm c}$. The most dangerous instability mode occurs for $k_{\rm max} = \sqrt{(k_{\rm c}^2 - M^0_{\rm nc}/M^0_{\rm c})/2}$ with $\beta_{\rm max} = M^0_{\rm c}\,\gamma\,(M^0_{\rm nc}/M^0_{\rm c} + k_{\rm c}^2)^2/4$ if the expression under the square root is positive. Otherwise the mode with $k = 0$ grows fastest ($\beta(k = 0) = M^0_{\rm nc} k_{\rm c}^2$).

The onset of instability occurs at $\partial_{\phi\phi} f|_{\phi=\phi_0} = 0$ with $k_{\rm c}^{\rm onset} = 0$, i.e. it is a long-wave instability. Qualitatively different examples of dispersion relations above and below the instability threshold are given in figure 4.

As above, steady thickness profiles are obtained by setting $\partial_t \phi = 0$ in equation (1). For a linearly unstable film a one-parameter family of profiles bifurcates from the flat film at $k_{\rm c}$ as illustrated in the four panels of figure 5. In contrast to the case without evaporation/condensation here the mean film thickness changes along the branches whereas the imposed chemical potential remains constant. A selection of film thickness profiles is given in figure 6.

Most notably the resulting branches always bifurcate supercritically from the trivial solution. The results furthermore indicate that there is no metastable film thickness range at all, implying that nucleation does not play any role for a condensing/evaporating film described by the present disjoining pressure. This, however, needs a deeper analysis in future, including a comparison of the behaviour for different pressure terms. Remarkably, the amplitude (droplet height) approaches a limiting value for a domain size of about $3L_{\rm c}/2$. As the energy monotonically decreases with domain size we expect these solutions to be unstable w.r.t. coarsening as the droplet pattern in the non-volatile case. Note finally that everything discussed above for non-volatile films regarding the infinite number of primary solution branches applies as well to the branches shown in figure 5.

After the short analysis of the volatile and non-volatile thin liquid film system we next focus on a thin film equation that describes the evolution of a solid film.

4. Epitaxial growth

The final example is a thin film model for the epitaxial evolution of surfaces of crystalline solids for a fixed amount of deposited material that is illustrated here employing a simplified 'glued wetting-layer model' [40]. The evolution equation (1) describes such a system when combined with the energy functional (4) and $M_{\rm nc} = 0$. As in the case of the non-volatile liquid film, material is conserved and any flat film of thickness $\phi = \phi_0$ corresponds to a steady state solution of the system.

As those trivial steady states might be unstable we perform a linear stability analysis along the lines of the previous sections and obtain the dispersion relation

$$\beta(k) = -M^0_{\rm c}\nu k^2(k^2 - k_{\rm c1}^2)\,(k^2 - k_{\rm c2}^2) \tag{8}$$

with

$$k_{\rm c1/c2} = \sqrt{\frac{\sigma}{2\nu}\left(1 \pm \sqrt{1 - \frac{4\nu\,\partial_{\phi\phi} f|_{\phi=\phi_0}}{\sigma^2}}\right)}. \tag{9}$$

The film is linearly unstable for $\partial_{\phi\phi} f|_{\phi=\phi_0} < \sigma^2/4\nu$ in the wavenumber range $k_{\rm c1} < k < k_{\rm c2}$. The fastest growing mode has the wavenumber $k_{\rm max} = (\sigma/3\nu)^{1/2}\sqrt{1 + \sqrt{1 - 3\nu\partial_{\phi\phi} f|_{\phi=\phi_0}/\sigma^2}}$. For values of $\partial_{\phi\phi} f|_{\phi=\phi_0} < 0$ one of the two critical wavenumbers becomes imaginary, i.e. the film is then unstable for $0 < k < k_{\rm c2}$. Note that the onset of the instability occurs at $\partial_{\phi\phi} f|_{\phi=\phi_0} = \sigma^2/4\nu$ with $k_{\rm c}^{\rm onset} = \sqrt{\sigma/2\nu}$, i.e. it is a short-wave instability. Qualitatively different examples of actual dispersion curves above and below the instability threshold are given in figure 7.

As in the other two cases steady thickness profiles are obtained by setting $\partial_t \phi = 0$ in equation (1). Here they do not represent profiles of liquid droplets, but profiles of solid quantum or nano-dots. Due to the higher-order terms in the energy (4) as compared to the functional (3) studied up to now, the dispersion curves (figure 7) are qualitatively quite different

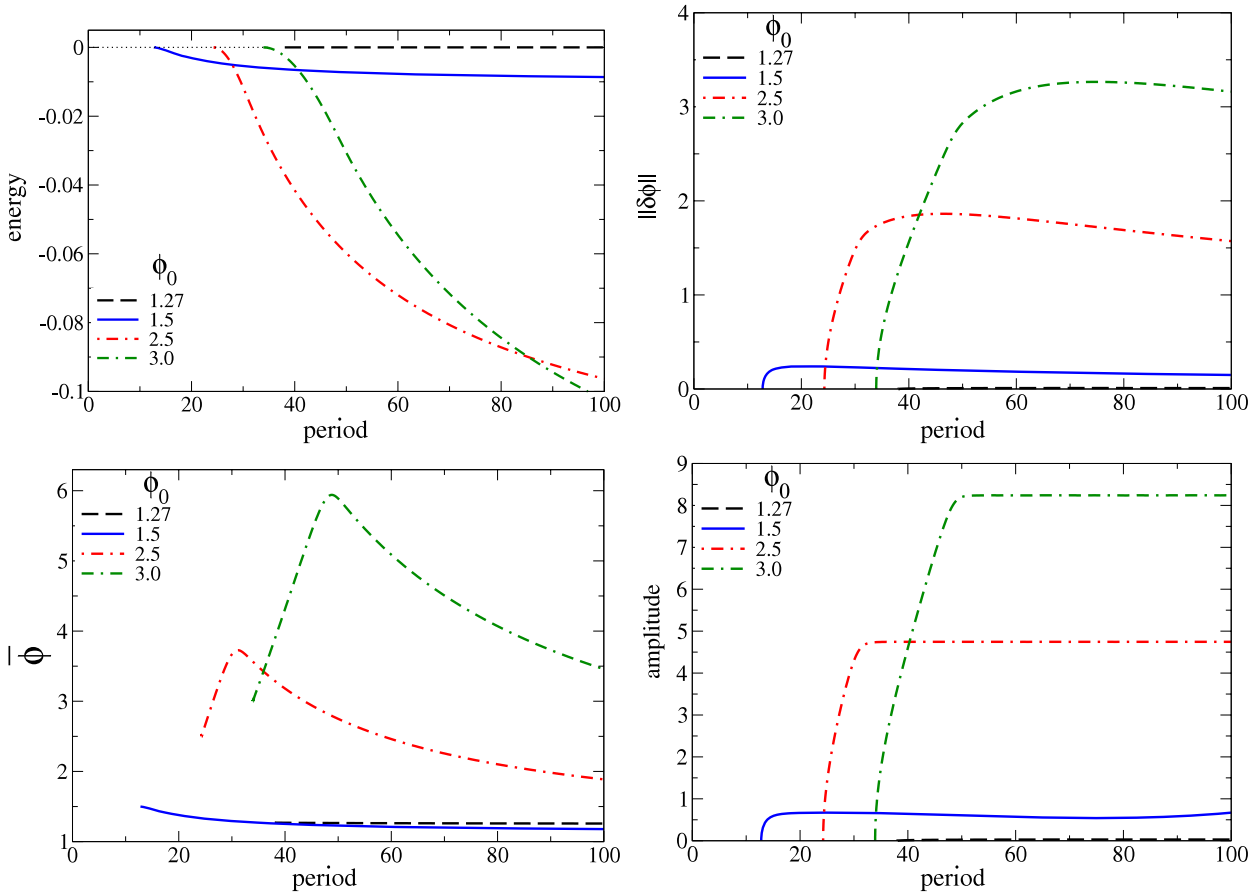

Figure 5. Shown are characteristics of families of steady one-dimensional droplet structures arising in dewetting of a volatile liquid using a simple disjoining pressure. From top left to bottom right the panels give the L_2-norm, the energy F (equation (3)) per length, the mean film thickness $\bar{\phi}$ and the droplet amplitude. The legends give the corresponding mean film thicknesses for the flat film ϕ_0 at the identical chemical potential μ. The families are obtained using continuation techniques. Note that the solutions are unstable w.r.t. coarsening.

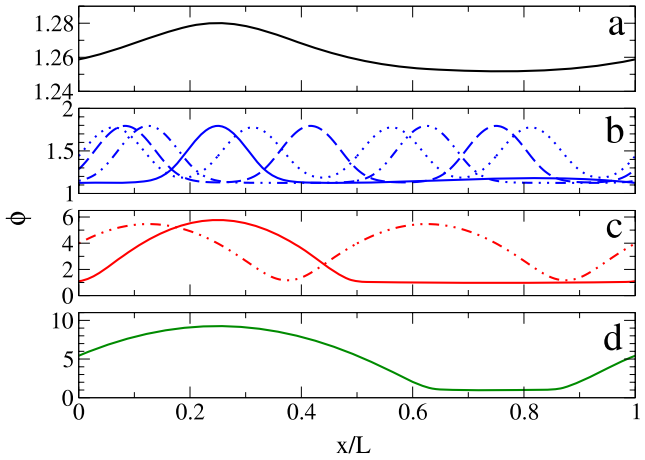

Figure 6. Shown are examples of film thickness profiles for the various branches presented in figure 5. Mean thicknesses $\bar{\phi}$ are (a) 1.27, (b) 1.5, (c) 2.5 and (d) 3.0. The system size is $L = 60$ in all cases. Given are profiles from the following branches: $n = 1$ (solid lines), $n = 2$ (dotted–dashed lines), $n = 3$ (dashed line) and $n = 4$ (dotted line).

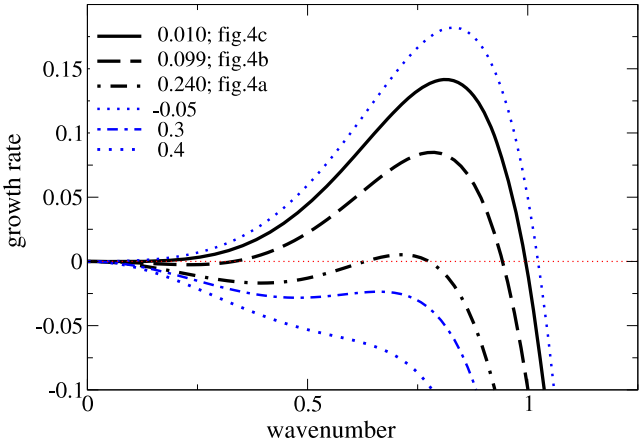

Figure 7. Dispersion relations for the instability of a flat epitaxial film w.r.t. surface modulations result in the growth of quantum dots. Used here is the simplest model proposed in [40]. The legend gives the dimensionless value of $\partial_\phi f$ at ϕ_0. Starting with the lowest one the three bold curves correspond to the cases studied in figures 4(a), (b) and (c) of [40].

from the ones for dewetting (figure 1). As a consequence we expect a rather different picture for the steady state solutions as well. At the parameter values allowing for two critical wavenumbers k_{c1} and k_{c2}, i.e. for $\partial_{\phi\phi} f|_{\phi=\phi_0} > 0$, one finds two bifurcations from the trivial solutions at domain sizes $2\pi/k_{c1}$ and $2\pi/k_{c2}$, respectively. Near onset one expects the two

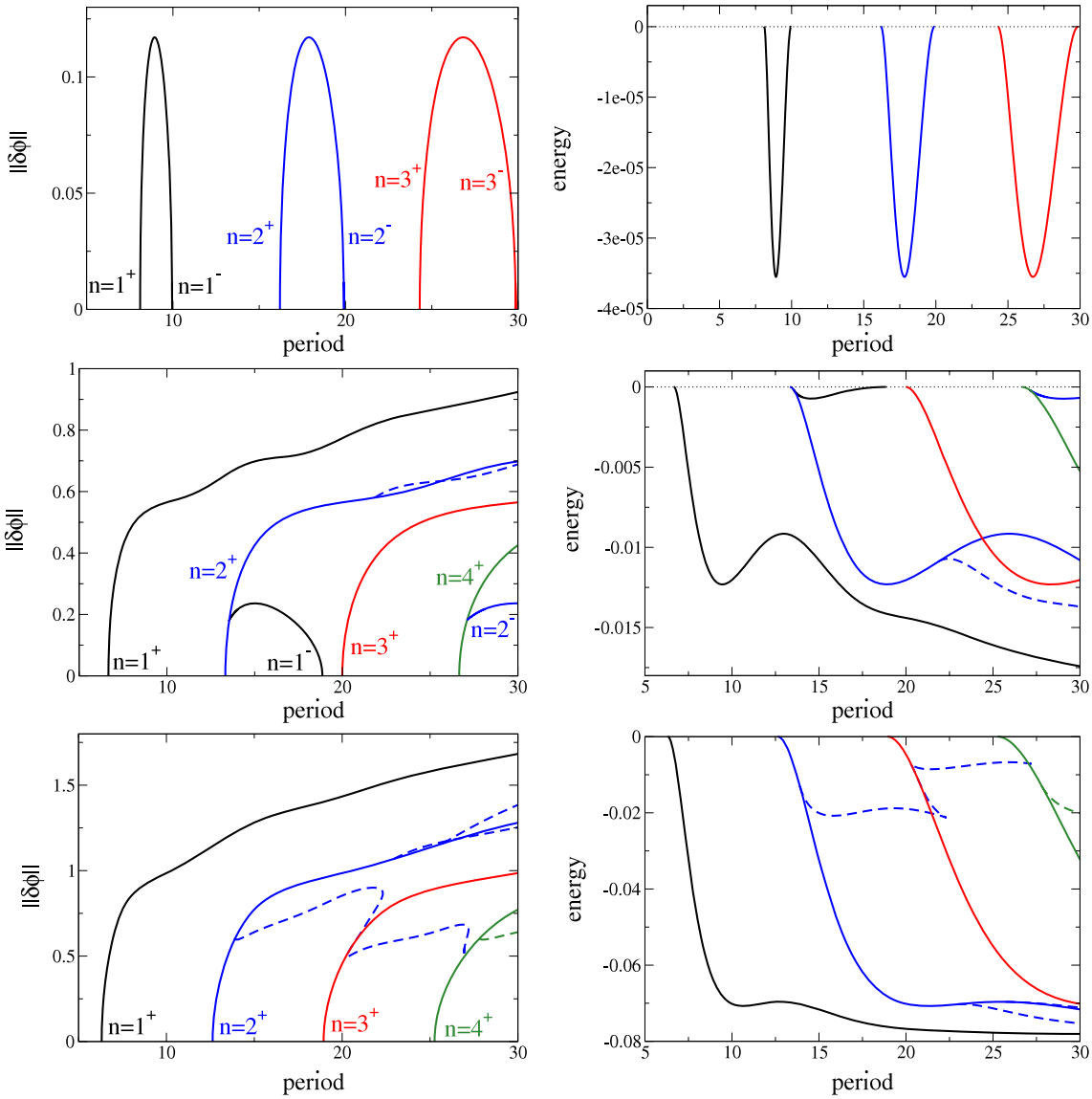

Figure 8. Shown are characteristics of families of steady one-dimensional surface structures (quantum dots) arising in epitaxial growth using the simplest model proposed in [40]. The panels in the left column give the L_2-norm and the ones in the right column the energy F (equation (4)) per length. Parameter values correspond to (top row) figure 4(a), (middle row) figure 4(b) and (bottom row) figure 4(c) of [40]. From top to bottom the non-dimensional wetting interaction increases, leading to more intricate behaviour. The families are obtained using continuation techniques.

emerging branches to interconnect, as at onset the solution space should change only locally. Further above onset the behaviour might, however, be dramatically different. The two branches bifurcating at $2\pi/k_{c1}$ and $2\pi/k_{c2}$ are the first of two infinite series of primary solution branches that bifurcate at respective domain sizes $L_{c1n} = 2\pi n/k_{c1}$ and $L_{c2n} = 2\pi n/k_{c2}$ with $n = 1, 2, \ldots$. This consideration is of importance here, as the various primary branches may actually couple.

We illustrate the solution structure in figure 8 using parameter values as in figure 4 of [40]. Shown are the norm (left column) and energy (right column) of the solutions on the various branches for three (positive) values of the strength of the wetting interaction. A selection of film thickness profiles is given in figure 9. As the strength of the wetting interaction decreases the system gets deeper into the unstable regime and the behaviour becomes more intricate. In the upper row of figure 8 we are slightly above onset and the two $n = 1$ branches that emerge at the two zero crossings of the dispersion relation actually connect, as expected. They are well separated from the branches with $n > 1$. Single-quantum-dot ($n = 1$) solutions only exist for a small range of periods $L_{c1} < L < L_{c2}$, i.e. the system is not able to undergo any coarsening. This corresponds well to the results obtained in [40] using weakly nonlinear analysis and integration in time. In the following we will call the branch emerging at $i\,L_{c1}$ [$i\,L_{c2}$] the left [right] $n = i$ branch.

The picture changes, however, further above onset, i.e. when decreasing the wetting interactions (middle row of figure 8). The two $n = 1$ branches do not interconnect any more. Actually, the left $n = 1$ branch continues towards $L = \infty$ without any side branches. The left $n = 2$ branch may change its stability with respect to coarsening with increasing domain size. Every time it changes stability

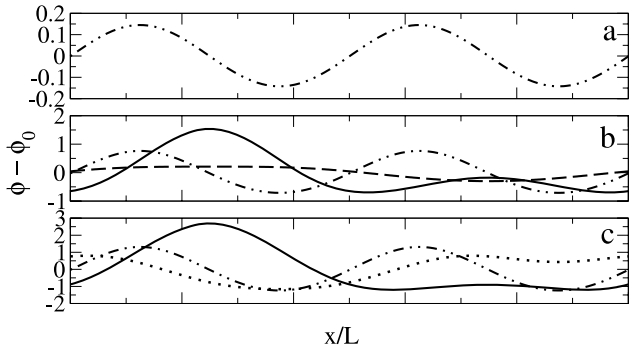

Figure 9. Shown are examples of film thickness profiles ($\phi - \phi_0$) for the various branches presented in figure 8. The parameters correspond to (a) the top row, (b) the middle row and (c) the bottom row of figure 8. The chosen system size is $L = 17$ in all cases. Given are profiles from the $n = 1^+$ branch (solid lines), the $n = 2^+$ branch (dotted–dashed lines), the $n = 1^-$ branch (dashed line in (b)) and the first side branch of the $n = 2^+$ branch (dotted line in (c)) as defined in figure 8. Mean film thickness is $\phi_0 = 1.75$.

a secondary branch bifurcates in a period doubling bifurcation rather similar to the scenario described for driven liquid films on inclined plates [34]. The right $n = 1$ branch connects via one of the branching points to the left $n = 2$ branch. The behaviour becomes increasingly involved for higher branch numbers.

Decreasing the wetting interaction even more brings the system further above threshold (bottom row of figure 8). As k_{c1} becomes quite small the right $n = 1$ branch bifurcates at very large domain sizes. However, the first secondary branch of the left $n = 2$ branch now splits up into various pieces that connect different left branches via secondary bifurcations.

We will at present not go deeper into the analysis. In particular, no proper stability analysis for the steady states is done here and, as above, for the dewetting system time evolution is not touched. Simulations can be found, for instance, in [42, 40, 2, 44–46]. Note that the results on stability sketched in the previous paragraph are inferred from the structure of the bifurcation diagrams alone. They need to be scrutinized in detail as they are very important for the coarsening behaviour. The non-monotonic dependence of energy on system size in figure 8 indicates that coarsening will depend on structure length in a non-trivial way. The long-time coarsening for epitaxial growth is discussed, for example, in [93–95].

The results presented for the glued wetting-layer model indicate that our knowledge about epitaxial growth would benefit from a more detailed analysis that maps out the steady solutions and their stability systematically for the various models proposed in the literature. Numerical techniques are available to do this not only for two-dimensional but for three-dimensional systems as well [50].

5. Conclusion

In the present contribution we have applied a basic mathematical analysis to three different physical systems involving solid and liquid films at solid surfaces that may undergo a structuring process by dewetting, evaporation/condensation or epitaxial growth, respectively. The aim has been to highlight similarities and differences of the three systems based on the observation that all of them can be described using models of similar form, i.e. a time evolution equation for a purely dissipative system without any inertia based on a gradient dynamics that is characterized by mobility functions and an underlying energy functional. Thereby the dynamics might have a non-conserved and/or conserved part. Equations like the well-known Cahn–Hilliard (purely conserved) and Allen–Cahn (purely non-conserved) equations represent limiting cases (with respect to the chosen dynamics) of this general evolution equation. They are normally used with a particularly simple form of the energy functional as well.

The three physical systems discussed here all fit into the general framework when choosing different mobilities and/or energy functionals. Beside the mathematical similarity the systems as well model similar physical phenomena as the respective liquid and solid films structure under the influence of their effective interactions with the substrate. However, although most readers will agree that the epitaxial growth of quantum dots is a subject of surface science, less of them might do so in the case of a dewetting liquid film. We hope that our review contributes to the development of a more unified view onto these processes of self-organization at interfaces.

In particular, we have used two basic steps of mathematical analysis, namely the study of the linear stability of homogeneous steady states, i.e. flat films, and the mapping of non-trivial steady states, i.e. drop/hole (quantum-dot) in dependence on system size for various values of interaction constants and/or mean film thickness. Our aim has been to illustrate that the underlying solution structure might be very complex as in the case of epitaxial growth but can be understood better when comparing to the much simpler results for the dewetting liquid film. We have furthermore shown that the continuation techniques employed can shed some light on this structure in a more convenient way than time-stepping methods. One might further argue that understan ding the solution structure of the quantum-dot system might as well allow us to predict pathways of evolution in time for an epitaxial layer as the behaviour will ultimately be determined by the steady solutions and their stability. This procedure was already followed for thin liquid films [74, 71, 96].

The usage of a general formulation like equation (1) does not only relate seemingly unrelated physical systems mathematically. It does as well allow us to discuss model extensions in a more unified way. Taking epitaxial growth as an example, the general form (1) would propose that in the non-conserved case, i.e. when material is deposited from the gas phase continuously the non-conserved part of the equation should be $-M_{nc}\delta F/\delta\phi$ with F given by (4). The constant deposition often used in the literature would then only refer to the limit of a rather large chemical potential. Oblique deposition of material [38] might as well be modelled incorporating, besides the vertical influx, lateral driving contributions as well.

The formulation reviewed here can be extended in a straightforward way to the case of N coupled fields

$\boldsymbol{\phi} = (\phi_1, \phi_2, \ldots, \phi_N)$ following a gradient dynamics that is governed by an energy functional $F[\phi_1, \phi_2, \ldots, \phi_N]$. The evolution equation is

$$\partial_t \boldsymbol{\phi} = \nabla \cdot \left[\underline{\mathbf{M}}_{\mathrm{c}} \cdot \nabla \frac{\delta F}{\delta \boldsymbol{\phi}} \right] - \underline{\mathbf{M}}_{\mathrm{nc}} \cdot \frac{\delta F}{\delta \boldsymbol{\phi}} \tag{10}$$

with the $\underline{\mathbf{M}}_{\mathrm{c}}(\boldsymbol{\phi}) \geqslant 0$ and $\underline{\mathbf{M}}_{\mathrm{nc}}(\boldsymbol{\phi}) \geqslant 0$ being symmetric positive-definite mobility matrices for the conserved and non-conserved parts of the dynamics, respectively. They are formed by $N \times N$ mobility functions, respectively. Note that $\delta F/\delta \boldsymbol{\phi}$ corresponds to a vector of dimension N. A typical example is the evolution of a dewetting two-layer system where the ϕ_1 and ϕ_2 correspond to the two film thicknesses, respectively. The formulation as a special case of (10) is derived from the Navier–Stokes equations in the two liquid layers and appropriate boundary conditions for spatially two- and three-dimensional settings in [96–99]. The formulation in the form of equation (10) has the advantage that one can easily check the consistency of the mobility functions after a normally rather involved derivation. Furthermore one can draw on rather general results, e.g. for the linear stability of flat film solutions [97]. Note that such a formulation will apply to any multi-layer system in a relaxational setting, including films of dielectric liquids in a capacitor [100, 101] or multi-layer pending films under the influence of gravity. We expect it to hold as well for the relaxation dynamics of multi-layer epitaxial films.

Let us finally note that we have entirely excluded spatially heterogeneous systems, i.e. systems described by equations of form (1) where the energy depends explicitly on position. Such systems are already treated for dewetting films [102–104, 17, 82, 71]: however, we are not aware of any such studies for epitaxial growth. We have as well excluded laterally driven systems described by equations like (1) that additionally include lateral driving forces. A comparison of sliding droplets on an incline [88, 34], a driven (or convective) Cahn–Hilliard system [79] and epitaxial growth under oblique deposition might be rather interesting, for instance, in terms of coarsening behaviour [105, 106, 34, 94]. The combination of both effects, i.e. heterogeneous systems with lateral driving, allows us to describe the depinning and stick–slip motion of droplets [92, 107]. The problems has, up to now, however, no counterpart in epitaxial growth.

References

[1] Ghoniem N and Walgraef D D 2008 *Instabilities and Selforganisation in Materials* (Oxford: Oxford University Press)
[2] Vvedensky D D 2004 *J. Phys.: Condens. Matter* **16** R1537
[3] Langer J S 1992 *Solids far from Equilibrium* ed C Godreche (Cambridge: Cambridge University Press) pp 297–363
[4] Cahn J W and Hilliard J E 1958 *J. Chem. Phys.* **28** 258
[5] Cahn J W 1965 *J. Chem. Phys.* **42** 93
[6] de Gennes P-G 1985 *Rev. Mod. Phys.* **57** 827
[7] Israelachvili J N 1992 *Intermolecular and Surface Forces* (London: Academic)
[8] Mitlin V S 1993 *J. Colloid Interface Sci.* **156** 491
[9] Oron A, Davis S H and Bankoff S G 1997 *Rev. Mod. Phys.* **69** 931
[10] Pismen L M and Pomeau Y 2000 *Phys. Rev.* E **62** 2480
[11] Kalliadasis S and Thiele U (ed) 2007 *Thin Films of Soft Matter* (Wien: Springer) ISBN 978-3-211-69807-5, CISM 490
[12] Fetzer R, Jacobs K, Münch A, Wagner B and Witelski T P 2005 *Phys. Rev. Lett.* **95** 127801
[13] Lyushnin A V, Golovin A A and Pismen L M 2002 *Phys. Rev.* E **65** 021602
[14] Burelbach J P, Bankoff S G and Davis S H 1988 *J. Fluid Mech.* **195** 463
[15] Oron A and Bankoff S G 1999 *J. Colloid Interface Sci.* **218** 152
[16] Schwartz L W, Roy R V, Eley R R and Petrash S 2001 *J. Colloid Interface Sci.* **214** 363
[17] Kargupta K, Konnur R and Sharma A 2001 *Langmuir* **17** 1294
[18] Bestehorn M and Merkt D 2006 *Phys. Rev. Lett.* **97** 127802
[19] Dzyaloshinskii I E, Lifshitz E M and Pitaevskii L P 1960 *Sov. Phys.—JETP* **37** 161
[20] Ruckenstein E and Jain R K 1974 *J. Chem. Soc. Faraday Trans.* II **70** 132
[21] Hocking L M 1993 *Phys. Fluids* A **5** 793
[22] Sharma A and Khanna R 1998 *Phys. Rev. Lett.* **81** 3463
[23] Eres M H, Schwartz L W and Roy R V 2000 *Phys. Fluids* **12** 1278
[24] Thiele U, Velarde M G, Neuffer K and Pomeau Y 2001 *Phys. Rev.* E **64** 031602
[25] Lin Z, Kerle T, Baker S M, Hoagland D A, Schäffer E, Steiner U and Russell T P 2001 *J. Chem. Phys.* **114** 2377
[26] Lin Z, Kerle T, Russell T P, Schäffer E and Steiner U 2002 *Macromolecules* **35** 3971
[27] Verma R, Sharma A, Kargupta K and Bhaumik J 2005 *Langmuir* **21** 3710
[28] John K and Thiele U 2007 *Appl. Phys. Lett.* **90** 264102
[29] John K, Hänggi P and Thiele U 2008 *Soft Matter* **4** 1183
[30] Oron A and Rosenau P 1994 *J. Fluid Mech.* **273** 361
[31] Golovin A A, Nepomnyashchy A A and Pismen L M 1994 *Phys. Fluids* **6** 34
[32] Oron A 2000 *Phys. Rev. Lett.* **85** 2108
[33] Bestehorn M, Pototsky A and Thiele U 2003 *Eur. Phys. J.* B **33** 457
[34] Thiele U and Knobloch E 2004 *Physica* D **190** 213
[35] Merkt D, Pototsky A, Bestehorn M and Thiele U 2005 *Phys. Fluids* **17** 064104
[36] Novick-Cohen A and Segel L A 1984 *Physica* D **10** 277
[37] Frastia L, Pismen L and Thiele U 2009 submitted
[38] Spencer B J, Voorhees P W and Davis S H 1991 *Phys. Rev. Lett.* **67** 3696
[39] Savina T V, Golovin A A, Davis S H, Nepomnyashchy A A and Voorhees P W 2003 *Phys. Rev.* E **67** 021606
[40] Golovin A A, Levine M S, Savina T V and Davis S H 2004 *Phys. Rev.* B **70** 235342
[41] Golovin A A, Davis S H and Nepomnyashchy A A 1999 *Phys. Rev.* E **59** 803
[42] Siegert M 1997 *Physica* A **239** 420
[43] Haataja M, Muller J, Rutenberg A D and Grant M 2002 *Phys. Rev.* B **65** 165414
[44] Pang Y Y and Huang R 2006 *Phys. Rev.* B **74** 075413
[45] Pang Y Y and Huang R 2007 *J. Appl. Phys.* **101** 023519
[46] Tekalign W T and Spencer B J 2007 *J. Appl. Phys.* **102** 073503
[47] Doedel E, Keller H B and Kernevez J P 1991 *Int. J. Bifurcation Chaos* **1** 493
[48] Doedel E, Keller H B and Kernevez J P 1991 *Int. J. Bifurcation Chaos* **1** 745
[49] Doedel E J, Champneys A R, Fairgrieve T F, Kuznetsov Y A, Sandstede B and Wang X J 1997 *AUTO97: Continuation and Bifurcation Software for Ordinary Differential Equations* (Montreal: Concordia University)

[50] Beltrame P and Thiele U 2009 submitted
[51] Anderson D M, McFadden G B and Wheeler A A 1998 *Annu. Rev. Fluid Mech.* **30** 139
[52] Wise S M, Lowengrub J S, Kim J S and Johnson W C 2004 *Superlattices Microstruct.* **36** 293
[53] Rabani E, Reichman D R, Geissler P L and Brus L E 2003 *Nature* **426** 271
[54] Yosef G and Rabani E 2006 *J. Phys. Chem.* B **110** 20965
[55] Vancea I, Thiele U, Pauliac-Vaujour E, Stannard A, Martin C P, Blunt M O and Moriarty P J 2008 *Phys. Rev.* E **78** 041601
[56] Vicsek T 1989 *Fractal Growth Phenomena* 1st edn (Singapore: World Scientific)
[57] Hinrichsen H 2006 *Physica* A **369** 1
[58] Reiter G 1992 *Phys. Rev. Lett.* **68** 75
[59] Seemann R, Herminghaus S, Neto C, Schlagowski S, Podzimek D, Konrad R, Mantz H and Jacobs K 2005 *J. Phys.: Condens. Matter* **17** S267
[60] Thiele U, Mertig M and Pompe W 1998 *Phys. Rev. Lett.* **80** 2869
[61] Martin C P, Blunt M O, Pauliac-Vaujour E, Stannard A, Moriarty P, Vancea I and Thiele U 2007 *Phys. Rev. Lett.* **99** 116103
[62] Pismen L M 2001 *Phys. Rev.* E **6402** 021603
[63] Pismen L M and Pomeau Y 2004 *Phys. Fluids* **16** 2604
[64] Pismen L M and Thiele U 2006 *Phys. Fluids* **18** 042104
[65] Thiele U, Velarde M G, Neuffer K, Bestehorn M and Pomeau Y 2001 *Phys. Rev.* E **64** 061601
[66] Teletzke G F, Davis H T and Scriven L E 1988 *Rev. Phys. Appl.* **23** 989
[67] Oron A and Rosenau P 1992 *J. Physique* II **2** 131
[68] Sharma A 1993 *Langmuir* **9** 3580
[69] Sharma A and Reiter G 1996 *J. Colloid Interface Sci.* **178** 383
[70] Thiele U, Neuffer K, Pomeau Y and Velarde M G 2002 *Colloids Surf.* A **206** 135
[71] Thiele U, Brusch L, Bestehorn M and Bär M 2003 *Eur. Phys. J.* E **11** 255
[72] John K, Bär M and Thiele U 2005 *Eur. Phys. J.* E **18** 183
[73] Thiele U, Vega J M and Knobloch E 2006 *J. Fluid Mech.* **546** 61
[74] Thiele U, Velarde M G and Neuffer K 2001 *Phys. Rev. Lett.* **87** 016104
[75] Becker J, Grün G, Seemann R, Mantz H, Jacobs K, Mecke K R and Blossey R 2003 *Nat. Mater.* **2** 59
[76] Thiele U 2003 *Eur. Phys. J.* E **12** 409
[77] Diez J A and Kondic L 2007 *Phys. Fluids* **19** 072107
[78] Beltrame P, Hänggi P and Thiele U 2009 submitted
[79] Golovin A A, Nepomnyashchy A A, Davis S H and Zaks M A 2001 *Phys. Rev. Lett.* **86** 1550
[80] Thiele U, Madruga S and Frastia L 2007 *Phys. Fluids* **19** 122106
[81] Bertozzi A L, Grün G and Witelski T P 2001 *Nonlinearity* **14** 1569
[82] Brusch L, Kühne H, Thiele U and Bär M 2002 *Phys. Rev.* E **66** 011602
[83] Glaser K B and Witelski T P 2003 *Phys. Rev.* E **67** 016302
[84] Glasner K B and Witelski T P 2005 *Physica* D **209** 80
[85] Torcini A and Politi P 2002 *Eur. Phys. J.* B **25** 519
[86] Kohn R V and Otto F 2002 *Commun. Math. Phys.* **229** 375
[87] Bestehorn M and Neuffer K 2001 *Phys. Rev. Lett.* **87** 046101
[88] Thiele U, Neuffer K, Bestehorn M, Pomeau Y and Velarde M G 2002 *Colloids Surf.* A **206** 87
[89] Pereira A, Trevelyan P M J, Thiele U and Kalliadasis S 2007 *Phys. Fluids* **19** 112102
[90] Thiele U and Knobloch E 2003 *Phys. Fluids* **15** 892
[91] Scheid B, Ruyer-Quil C, Thiele U, Kabov O A, Legros J C and Colinet P 2005 *J. Fluid Mech.* **527** 303
[92] Thiele U and Knobloch E 2006 *New J. Phys.* **8** 313 1
[93] Siegert M 1998 *Phys. Rev. Lett.* **81** 5481
[94] Watson S J and Norris S A 2006 *Phys. Rev. Lett.* **96** 176103
[95] Leo P H and Johnson W C 2001 *Acta Mater.* **49** 1771
[96] Pototsky A, Bestehorn M, Merkt D and Thiele U 2004 *Phys. Rev.* E **70** 025201(R)
[97] Pototsky A, Bestehorn M, Merkt D and Thiele U 2005 *J. Chem. Phys.* **122** 224711
[98] Fisher L S and Golovin A A 2005 *J. Colloid Interface Sci.* **291** 515
[99] Pototsky A, Bestehorn M, Merkt D and Thiele U 2006 *Europhys. Lett.* **74** 665
[100] Bandyopadhyay D, Gulabani R and Sharma A 2005 *Ind. Eng. Chem. Res.* **44** 1259
[101] Bandyopadhyay D and Sharma A 2007 *J. Colloid Interface Sci.* **311** 595
[102] Lenz P and Lipowsky R 1998 *Phys. Rev. Lett.* **80** 1920
[103] Bauer C, Dietrich S and Parry A O 1999 *Europhys. Lett.* **47** 474
[104] Konnur R, Kargupta K and Sharma A 2000 *Phys. Rev. Lett.* **84** 931
[105] Emmott C L and Bray A J 1996 *Phys. Rev.* E **54** 4568
[106] Watson S J, Otto F, Rubinstein B Y and Davis S H 2003 *Physica* D **178** 127
[107] Thiele U and Knobloch E 2006 *Phys. Rev. Lett.* **97** 204501